The 14th World Conference on Earthquake Engineering
October 12-17, 2008, Beijing, China

STUDY OF THE STABILITY AND ACCURACY OF A NONCONVOLUTIONAL, SPLIT-FIELD PERFECTLY MATCHED LAYER (PML) FOR WAVE PROPAGATION IN ELASTIC MEDIA

Kristel C. Meza-Fajardo[1] and Apostolos S. Papageorgiou[2]

[1] *Professor, Dept. de Ingeniería Civil, Universidad Nacional Autónoma de Honduras, Tegucigalpa, Honduras*
[2] *Professor, Dept. of Civil Engineering, University of Patras, Patras, Greece*
Email: kcmeza@upatras.gr, papaga@upatras.gr

ABSTRACT :

The Perfectly Matched Layer (PML) model is a material boundary condition for wave propagation in unbounded domains. It consists of an absorbing layer of finite width that surrounds the physical domain of interest so that all outgoing waves are damped out irrespective of their frequency and direction of propagation. The main feature of the PML is that, before discretization it does not generate reflections at the interface separating the PML and the physical medium, however a small reflection is always present after discretization. The satisfactory performance of the PML has resulted in considerable work towards its implementation in several wave-like problems including elastic wave propagation. In the present work we propose and implement a non-convolutional, split-field PML, referred to as the Multi-Axial Perfectly Matched Layer (M-PML). The formulation is obtained by generalizing the '*classical*' PML to a medium in which damping profiles are specified in more than one direction. Under the hypothesis of small damping and using an eigenvalue sensitivity analysis based on first derivatives, we propose a method to study the stability of the M-PML and demonstrate that it is related to the ratios of the damping profiles. A general procedure for constructing stable M-PML models for elastic media is then obtained. The effectiveness of the M-PML and its advantages relative to the classical PML, are demonstrated by constructing stable terminations for both isotropic as well as anisotropic 2-D media. As a final step in our analysis, we present a quantitative assessment of the accuracy of the proposed M-PML.

KEYWORDS: absorbing boundary conditions, perfectly matched layer, seismic wave propagation

1. INTRODUCTION

The Perfectly Matched Layer (PML) model was introduced by Bérenger (1994) as a material boundary condition for electromagnetic wave propagation problems in unbounded domains. The main feature of the PML is that, in the case of the continuum, it does not generate reflections at the interface separating the absorbing layer and the physical medium, however a small reflection is always present after discretization. In its original version (we refer to this version as the '*classical* PML'), the field variables of the PML are split in non-physical components so as to make it possible to incorporate in the mathematical formulation the desired absorption. Due to the effectiveness of the PML in absorbing the radiation exiting the physical domain, the extra memory storage required in order to accommodate the increased number of field variables is usually counterbalanced by the savings that are achieved by reducing the size of the physical domain. However, there are still some instances for which the performance of the classical PML does not meet expectations. In the case of elastic waves in isotropic media, it has been reported (Festa *et al.*, 2005; Komatitsch and Martin, 2007) that instabilities appear in long (in time) simulations. In addition, Bécache *et al*. (2003) documented that exponentially growing solutions could appear in some models for anisotropic elastic media. It was initially thought (Kuzuoglu and Mittra, 1996) that the source of the dynamical instability of the classical PML could be attributed to the fact the constitutive parameters did not satisfy causality, and an alternative causal frequency-dependent PML, known as the *Convolutional Perfectly Matched Layer* (C-PML), was proposed. Later, Teixeira and Chew (1999) showed that the original Cartesian PML parameters do indeed satisfy causality and that the abovementioned conclusion (regarding causality) was reached base on a technical error related to the Kramers-Kronig equations. Subsequently, it was demonstrated (Bécache *et al*. 2004) that the C-PML for isotropic media does not suffer from instabilities. However, Komatitsch and Martin (2007) observed that the C-PML does not solve all the instability problems for PML models for anisotropic media. Despite all the work done on the subject, a comprehensive mathematical analysis of the PML is not yet available and the problem of developing a general method to construct stable PML terminations remains open.

2. THE M-PML FORMULATION

The elastodynamics problem is defined by Cauchy's equation of motion and the generalized Hooke's law:

$$\rho \frac{\partial^2 \mathbf{u}}{\partial t^2} = \nabla \cdot \mathbf{T}, \qquad \mathbf{T} = \mathbf{C} : \mathbf{E} \tag{2.1}$$

where, $\mathbf{u}(\mathbf{x}, t)$ is the displacement field, $\mathbf{x}$ is the position vector, $\mathbf{T}(\mathbf{x}, t)$ is the stress tensor, $\mathbf{E}(\mathbf{x}, t) = (1/2)[\nabla\mathbf{u} + (\nabla\mathbf{u})^T]$ is the strain tensor, $\rho(\mathbf{x})$ is the mass density and $\nabla = [\partial/\partial x \quad \partial/\partial y \quad \partial/\partial z]$. Suppose that the interface between the physical domain and the absorbing medium is a plane normal to the x-axis at $x = 0$. The half-space corresponding to $x < 0$ is the physical domain and the other half space corresponding to $x > 0$ is the PML medium. As stated by Komatitsch and Tromp (2003), the main idea of the classical PML is to construct a new wave equation which admits plane-wave solutions of the form $\mathbf{u} = \mathbf{A}\exp[-i(\mathbf{k} \cdot \mathbf{x} - \omega t) - \gamma_x k_x/\omega]$, where $\gamma_x(x) > 0$, $\mathbf{A}$ is the polarization vector, $i = \sqrt{-1}$, and ω is the circular frequency. The vector $\mathbf{k} = [k_x \quad k_y \quad k_z]$, known as the wavevector, gives the direction of propagation of the wave front and the additional factor $\exp(-\gamma_x k_x/\omega)$ modulates the amplitude of the wave resulting in waves that decay exponentially in the direction of increasing x. A general procedure to derive classical PML formulations for linear wave propagation problems, known as 'coordinate stretching' (Chew and Weedon, 1994) is based on the following transformation of the spatial variable:

$$\tilde{x} = x - i\gamma_x/\omega \tag{2.2}$$

Then, transformation (2.2) is used to derive a new operator $\nabla_{\tilde{\mathbf{x}}} = [\partial/\partial\tilde{x} \quad \partial/\partial y \quad \partial/\partial z]$ where $\partial/\partial\tilde{x} = (1 - i\, d_x/\omega)\, \partial/\partial x$. The function $d_x = \partial\gamma_x/\partial x$ is referred to as the *damping profile* and is specified to introduce attenuation. The new operator $\nabla_{\tilde{\mathbf{x}}}$ then replaces ∇ in system (2.1) to obtain the new wave equation. Note that when $d_x = 0$ the operator $\nabla_{\tilde{\mathbf{x}}}$ reduces to that of the elastic medium. Bérenger's method then consists of placing the PML medium next to the boundary of the physical domain, and to avoid reflections, the damping profile is selected to be zero at the interface and smoothly increase across the PML width. The treatment of the "*corner regions*" (where two or three PMLs overlap) is straightforward since its properties are just the superposition of the intersecting PMLs.

In a classical PML, only one damping profile, d_x, is specified to be a function of the space variable x, whereas the other two profiles (d_y and d_z) are set equal to zero. We propose to generalize the properties of the classical PML, by selecting *all three* damping profiles to be functions of the x–coordinate. The additional damping profiles d_y and d_z are set to be proportional to d_x as follows (Meza-Fajardo & Papageorgiou, 2008):

$$d_x = d_x^{(x)}(x), \qquad d_y = p^{(y/x)} d_x^{(x)}(x), \qquad d_z = p^{(z/x)} d_x^{(x)}(x) \tag{2.3}$$

and the constants $p^{(y/x)}$ and $p^{(z/x)}$ are referred to as the *ratios of the damping profiles*. Given that $d_x^{(x)}(x)$ vanishes at $x = 0$, all damping profiles vanish at $x = 0$ and consequently, the proposed medium, referred to as the *Multi-Axial Perfectly Matched Layer (M-PML)*, retains the non-reflection characteristics of a PML. The transformations to construct the M-PML equations using the coordinate stretching approach are the following:

$$\tilde{x} = x - i\gamma_x/\omega, \qquad \tilde{y} = y - i\, d_y^{(x)} y/\omega, \qquad \tilde{z} = z - i\, d_z^{(x)} z/\omega \tag{2.4}$$

As in the classical PML, for the corner regions the properties of the overlapping layers are simply superimposed.

3. STABILITY ANALYSIS

In this section we perform a stability analysis of the M-PML for isotropic as well as orthotropic elastic media. In particular, we study the stability of the solutions of the Partial Differential Equation which governs the motion of the M-PML. The stability analysis is performed for M-PML terminations for a 2-D homogeneous elastic orthotropic medium whose axes of symmetry coincide with the x and y axes. The equations governing the (P-SV) wave motion can be expressed as the following velocity-stress system:

$$\rho \frac{\partial}{\partial t}\begin{bmatrix} v_x \\ v_y \end{bmatrix} = \begin{bmatrix} \frac{\partial}{\partial x}T_{xx} + \frac{\partial}{\partial y}T_{yx} \\ \frac{\partial}{\partial x}T_{xy} + \frac{\partial}{\partial y}T_{yy} \end{bmatrix}, \qquad \frac{\partial}{\partial t}\begin{bmatrix} T_{xx} \\ T_{yy} \\ T_{xy} \end{bmatrix} = \begin{bmatrix} c_{11} & c_{12} & 0 & 0 \\ c_{12} & c_{22} & 0 & 0 \\ 0 & 0 & c_{33} & c_{33} \end{bmatrix} \begin{bmatrix} \frac{\partial v_x}{\partial x} \\ \frac{\partial v_y}{\partial y} \\ \frac{\partial v_y}{\partial x} \\ \frac{\partial v_x}{\partial y} \end{bmatrix} \tag{3.1}$$

After applying transformations (2.4) and splitting the velocity and stress fields, the system of equations for the M-PML can be obtained. It is furthermore assumed that the mass density ρ and damping profiles d_x and d_y have constant values (in this case we refer to d_x and d_y as '*damping coefficients*'), so as to make Fourier Analysis in space tractable. The transformed set of equations may be written as a 10×10 system [a detailed derivation may be found in Meza-Fajardo and Papageorgiou (2008)] that takes the following form:

$$\frac{\partial \mathbf{U}}{\partial t} = \mathbf{AU} \tag{3.2}$$

where:

$$\mathbf{U} = \iint_{-\infty}^{+\infty} \mathbf{\Psi}(x,y,t)\, exp\left(ik_x x + ik_y y\right) dxdy, \qquad \mathbf{\Psi} = \left[T_{xx}^{(x)}\ T_{yy}^{(x)}\ T_{xy}^{(x)}\ T_{xx}^{(y)}\ T_{yy}^{(y)}\ T_{xy}^{(y)}\ v_x^{(x)}\ v_y^{(x)}\ v_x^{(y)}\ v_y^{(y)}\right]^T,$$

$$\mathbf{A} = \begin{bmatrix} -d_x\mathbf{I}_3 & \mathbf{0}_{33} & ik_x\mathbf{C}^{(x)} & ik_x\mathbf{C}^{(x)} \\ \mathbf{0}_{33} & -d_y\mathbf{I}_3 & ik_y\mathbf{C}^{(y)} & ik_y\mathbf{C}^{(y)} \\ ik_x\mathbf{D}^{(x)} & ik_x\mathbf{D}^{(x)} & -d_x\mathbf{I}_2 & \mathbf{0}_{22} \\ ik_y\mathbf{D}^{(y)} & ik_y\mathbf{D}^{(y)} & \mathbf{0}_{22} & -d_y\mathbf{I}_2 \end{bmatrix}, \tag{3.3}$$

$\mathbf{0}_{nm}$ is the $n \times m$ zero matrix, $\mathbf{I}_n$ is the $n \times n$ identiy matrix, and

$$\mathbf{D}^{(x)} = \frac{1}{\rho}\begin{bmatrix} 1 & 0 & 0 \\ 0 & 0 & 1 \end{bmatrix}, \qquad \mathbf{D}^{(y)} = \frac{1}{\rho}\begin{bmatrix} 0 & 0 & 1 \\ 0 & 1 & 0 \end{bmatrix}, \qquad \mathbf{C}^{(x)} = \begin{bmatrix} c_{11} & 0 \\ c_{12} & 0 \\ 0 & c_{33} \end{bmatrix}, \qquad \mathbf{C}^{(y)} = \begin{bmatrix} 0 & c_{12} \\ 0 & c_{22} \\ c_{33} & 0 \end{bmatrix} \tag{3.4}$$

Since the coefficients of matrix $\mathbf{A}$ do not depend on the time variable, system (3.2) is a *time-invariant* or *autonomous* system. We can then apply the classical spectral stability criteria provided by the theory of linear dynamical systems [e.g., Hinrichsen and Pritchard, (2005)]. In particular, for the autonomous system (3.2), all solutions $\mathbf{U}(t)$ are composed of transients (and thus it is asymptotically stable) if all the eigenvalues $\{\sigma_i\}$ of $\mathbf{A}$ have *negative* real parts. Since an absorbing layer like the M-PML is designed to dissipate all energy exiting the physical domain, asymptotic stability for the M-PML is desired.

In the simple case of the *split* elastic (i.e., undamped) system, the constant coefficient matrix $\mathbf{A}^e$ (obtained by setting d_x and d_y equal to zero in $\mathbf{A}$) has the following set of eigenvalues:

$$\sigma_i^e = \left\{ \begin{array}{c} \pm\frac{i}{\sqrt{2}}\sqrt{\left(c_4k_y^2 + c_3k_x^2\right) + \sqrt{\left(c_4k_y^2 + c_3k_x^2\right)^2 - 4\left(c_1k_x^4 + c_2k_y^4 + c_5k_x^2k_y^2\right)}}, \\ \pm\frac{i}{\sqrt{2}}\sqrt{\left(c_4k_y^2 + c_3k_x^2\right) - \sqrt{\left(c_4k_y^2 + c_3k_x^2\right)^2 - 4\left(c_1k_x^4 + c_2k_y^4 + c_5k_x^2k_y^2\right)}}, \\ 0^{(6)} \end{array} \right\} \tag{3.5}$$

where $c_1 = c_{33}c_{11}/\rho^2$, $c_2 = c_{33}c_{22}/\rho^2$, $c_4 = (c_{22}+c_{33})/\rho$, $c_3 = (c_{11}+c_{33})/\rho$, $c_5 = (c_{11}c_{22} - c_{12}^2 - 2c_{12}c_{33})/\rho^2$, and the exponent in the zero eigenvalue denotes its multiplicity. It is evident from Eq. (3.5) that the real parts of all eigenvalues of the elastic system are zero. On the other hand, from the characteristic equation of matrix $\mathbf{A}$ of the *damped* system, two eigenvalues are obtained by inspection:

$$\sigma_1 = -d_x \qquad \sigma_2 = -d_y \tag{3.6}$$

These eigenvalues show that, when damping is introduced, two of the six eigenvalues of the undamped split-field system that are equal to zero move to the left half of the complex plane. Regarding the remaining eight eigenvalues of matrix $\mathbf{A}$, no closed form expressions could be found, since they are the roots of a polynomial of degree eight. However, we recall that in order to characterize the stability of the M-PML system, we need to know only the sign of the real part of the eigenvalues. We then perform an *eigenvalue sensitivity analysis* (Adhikari and Friswell 2001, Gallina 2003). If the values of the damping coefficient $d_x^{(x)}$ are small, a simple way to detect the direction of motion of the i-th eigenvalue is to evaluate its first derivative with respect to $d_x^{(x)}$ when $d_x^{(x)} = 0$. Because in the undamped case all eigenvalues σ_i^e have zero real part, if $\mathrm{Re}(d\sigma_i/dd_x^{(x)}) < 0$ for all i when $d_x^{(x)} = 0$, a small $d_x^{(x)}$ will induce motion of the eigenvalues towards the 'negative' half complex plane, causing the system to become asymptotically stable.

We derived exact expressions for the 'eigenderivatives' by applying implicit differentiation to the characteristic equation of matrix $\mathbf{A}$. The derivatives of the m-th eigenvalue with respect to $d_x^{(x)}$ (for a horizontal strip) and $d_y^{(y)}$ (for a vertical strip) evaluated at the origin are given by (Meza-Fajardo, 2007):

$$\left.\frac{d\sigma_m}{dd_x^{(x)}}\right|_{d_x^{(x)}=0} = -\frac{1}{\tilde{D}}\Big\{2\big(1+p^{(y/x)}\big)(\tilde{\sigma}_m^e)^4 + \big[c_3 n_x^2\big(1+2p^{(y/x)}\big) + c_4 n_y^2\big(2+p^{(y/x)}\big)\big](\tilde{\sigma}_m^e)^2 + 2\big(c_1 p^{(y/x)} n_x^4 + c_2 n_y^4\big) + c_5 n_x^2 n_y^2\big(1+p^{(y/x)}\big)\Big\} \tag{3.7}$$

$$\left.\frac{d\sigma_m}{dd_y^{(y)}}\right|_{d_y^{(y)}=0} = -\frac{1}{\tilde{D}}\Big\{2\big(1+p^{(x/y)}\big)(\tilde{\sigma}_m^e)^4 + \big[c_3 n_x^2\big(2+p^{(x/y)}\big) + c_4 n_y^2\big(1+2p^{(x/y)}\big)\big](\tilde{\sigma}_m^e)^2 + 2\big(c_1 n_x^4 + c_2 p^{(x/y)} n_y^4\big) + c_5 n_x^2 n_y^2\big(1+p^{(x/y)}\big)\Big\} \tag{3.8}$$

with

$$\tilde{D} = 4(\tilde{\sigma}_m^e)^4 + 3\big(c_3 n_x^2 + c_4 n_y^2\big)(\tilde{\sigma}_m^e)^2 + 2\big(c_1 n_x^4 + c_2 n_y^4 + c_5 n_x^2 n_y^2\big) \tag{3.9}$$

where $\sigma_m^e = |\mathbf{k}|\tilde{\sigma}_m^e$, n_x and n_y are the direction cosines of the wave vector (i.e., $k_x = |\mathbf{k}|n_x$, $k_y = |\mathbf{k}|n_y$), and σ_m^e is the m-th eigenvalue of the undamped system. It becomes clear that the eigenderivatives (3.7) and (3.8) are determined by the elastic constants, the direction of propagation, *and by the ratios* $p^{(y/x)}$ and $p^{(x/y)}$, respectively. In Figure 1 these derivatives have been plotted as a function of the angle of incidence θ. Figures (1a) and (1b) correspond to the eigenderivatives for the classical PML whereas Figures (1c) and (1d) show the derivatives for the M-PML with $p^{(y/x)} = p^{(x/y)} = 0.1$. Clearly, if the ratios of damping coefficients are non-zero, the eigenderivatives (3.7) and (3.8) are negative for all directions of propagation, therefore the real part of the eigenvalues $\{\sigma_m\}$ is negative and consequently the M-PML for isotropic media is asymptotically stable. On the other hand, if the ratios of damping coefficients are zero (classical PML), the derivatives (3.7) and (3.8) will be zero for waves propagating parallel to either the x-axis, or to the y-axis, as figures (1a) and (1b) show. Consequently, the classical PML medium it is not asymptotically stable.

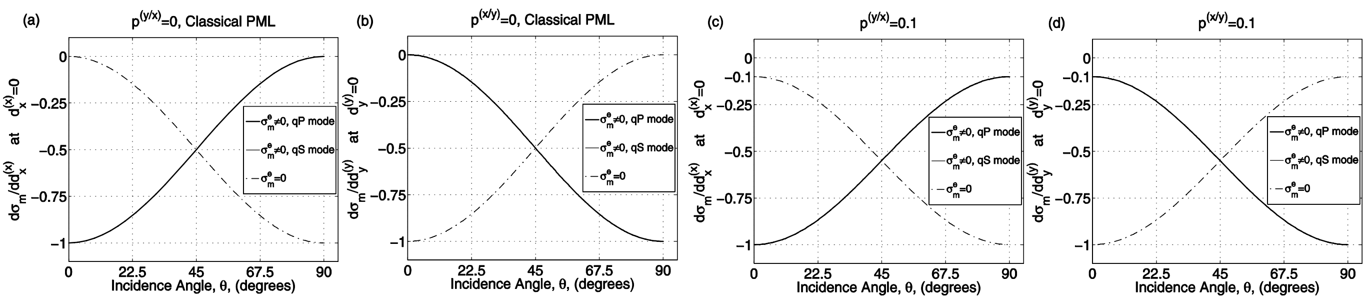

Figure 1. M-PML eigenderivatives for *isotropic* elastic media. Figures (a) and (b) correspond to the classical PML. Figures (c) and (d) correspond to the M-PML with $p^{(y/x)} = p^{(x/y)} = 0.1$ (from Meza-Fajardo & Papageorgiou, 2008).

Now we turn our attention to classical PML for more general orthotropic media. In particular, we consider the model for zinc reported by Komatitsch and Martin (2007), with elastic constants $c_{11} = 1.65\text{E}+11$ N/m^2, c_{22} = 6.20E+10 N/m^2, c_{33} =3.96E+10 N/m^2, c_{12} =5.00E+10 N/m^2. Figures (2a) and (2b) show that eigenderivatives corresponding to the qS mode for classical PML model can take positive values. As it can be observed in Figures (2c) and (2d), a value of $p^{(x/y)} = 0.1$ stabilizes the horizontal termination strip. For the vertical termination strip to become asymptotically stable, however, $p^{(y/x)} = 0.15$ seems to be the proper value, as Figure (2c) indicates.

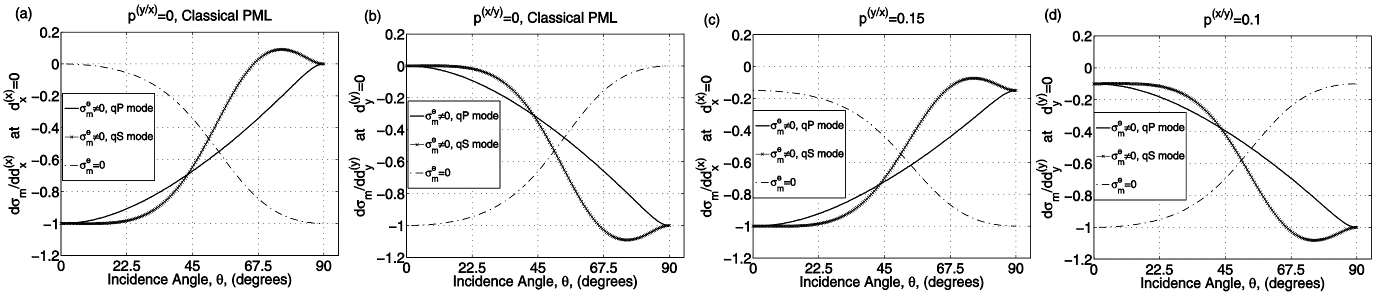

Figure 2. M-PML eigenderivatives for an orthotropic elastic medium (*Model for zinc*). Figures (a) and (b) correspond to the classical PML (c) M-PML with $p^{(y/x)} = 0.15$. (d) M-PML with $p^{(x/y)} = 0.1$ (from Meza-Fajardo & Papageorgiou, 2008).

4. NUMERICAL SIMULATIONS

The equations in the physical domain and M-PML terminations were discretized and solved in variational form with the Spectral Element Method (SEM). For implementation of the split-field M-PML in the SEM, the staggered velocity-stress time scheme proposed by Festa and Vilotte (2005) was adopted. For the simulations, we selected a quadratic damping profile of the form $d_x^{(x)} = d_0(x/H)^2$, $d_y^{(y)} = d_0(y/H)^2$, where H is the thickness of the absorbing termination strip and the parameter d_0 is the maximum value of the damping profile in the strip. The source time variation is given by a Ricker wavelet.

If simulations in elastic isotropic media are performed for long time durations, the multiple-zero instability inherent in the classical PML often arises and pollutes the solution in the physical domain. It has been reported (Festa et al. 2005) that implementation of the C-PML eliminates such instability. Here we show that the M-PML is also an efficient alternative solution. For demonstration purposes we consider the problem of the propagation of a P-wave in an isotropic elongated domain. The rectangular domain is terminated by absorbing layers on its four sides. The dimensions and properties of the media and discretization parameters are listed in Table 1. The maximum value of the damping profiles is given by $d_0 = Av_p/H$ (Festa and Vilotte, 2005), with A = 20. For comparison purposes, we performed the simulations with classical PML, M-PML with $p^{(y/x)} = p^{(x/y)} = 0.1$ and C-PML terminations. For the latter we adopted the same damping profile and a cut-off frequency of 0.8 Hz.

Table 1. Properties and discretization parameters for simulation in isotropic medium.

Physical domain dimensions			**Ricker wavelet parameters**		
Length	9	km	Dominant frequency	10	Hz
Width	0.8	km	Onset time	0.1	s
Physical domain properties			**Discretization parameters**		
Density	2.5E+12	kg/km^3	Polynomial degree	5	
S-wave velocity	2.31	km/s	Element side	0.05	km
P-wave velocity	4	km/s	Elements along PML width	8	
Source location			Time step	0.0003	s
From left boundary	0.3	km	Total duration	3	s
From bottom boundary	0.3	km			

In Figure 3 snapshots of the results are displayed for different instants of time. The interfaces between the physical domain and termination strips are represented by the solid lines. It can be observed that the body waves are well absorbed by the three termination strips. At t=2.3 sec the instability of the classical PML is visible. If the simulation is performed for longer times, the instability grows and spreads into the physical domain. No instabilities are identified in the C-PML and M-PML terminations.

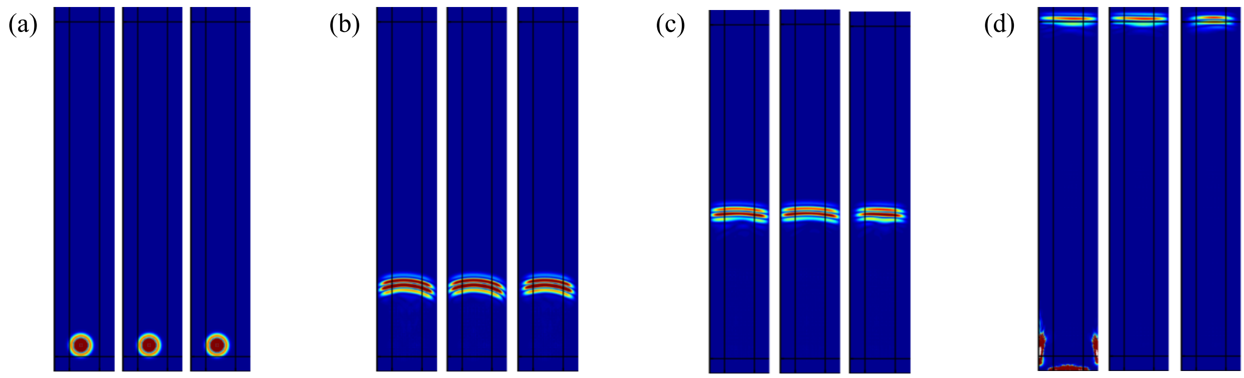

Figure 3. Snapshots of the propagation of the velocity magnitude of a *P*-wave generated by an explosive line source on an elongated domain surrounded by classical PML (left), C-PML (center) and M-PML (right) terminations at (a) 0.1 s, (b) 0.5 s, (c) 1 s, (d) 2.3 s (from Meza-Fajardo, 2008).

With the following numerical experiment we illustrate that it is possible to construct stable M-PMLs for orthotropic media as zinc. The configuration of the test is similar to that one presented by Komatitsch and Martin (2007). The physical domain is a square surrounded by M-PMLs on its four sides. The source is a concentrated vertical force acting at the center of the physical domain. The maximum value of damping d_0 adopted for this test is 0.47. Table 2 provides more details on the properties of the medium. Snapshots of the results of the numerical experiments at different times are displayed in Figure 4. It can be observed that both the *qP* and *qS* waves are well absorbed by both layers, namely, the classical PML and the M-PML with $p^{(y/x)} = p^{(x/y)} = 0.15$. At time instant t=400 μs the exponential growth is visible in both the vertical and the horizontal Classical PM strips (Figure 4d, upper row). On the other hand, no instabilities are detected in the snapshots for the M-PML terminations (Figure 4d, lower row).

Table 2. Properties and discretization parameters for simulation in Zinc.

Physical domain dimensions			**Ricker wavelet parameters**		
Length	25	cm	Dominant frequency	170	kHz
Width	25	cm	Onset time	5.88	μs
Physical domain properties			**Discretization parameters**		
Density	7100	kg/m^3	Polynomial degree	5	
c_{11}	1.65E+11	N/m^2	Element side	0.625	cm
c_{22}	6.20E+10	N/ m^2	Elements along PML width	10	
c_{33}	3.96E+10	N/ m^2	Time step	0.04	μs
c_{12}	5.00E+10	N/ m^2	Total duration	400	μs
Source location					
From left boundary	12.5	cm			
From bottom boundary	12.5	cm			

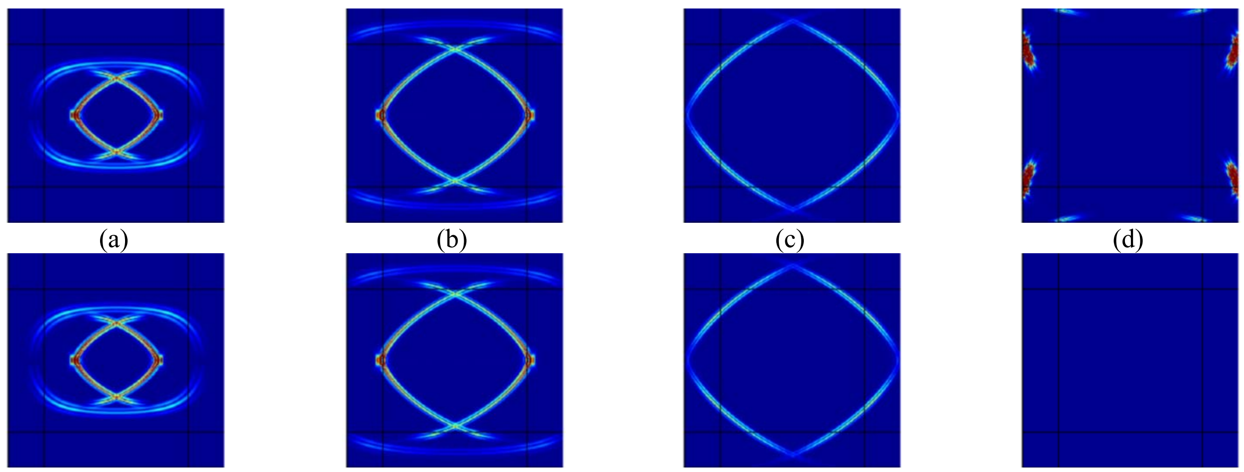

Figure 4. Snapshots of propagation of the velocity magnitude in orthotropic elastic medium, *Zinc Model*, at (a) t=35 µs, (b) t=60 µs, (c) t=85 µs, (d) t=400 μs. The top and bottom rows correspond to classical PML, and M-PML (with $p^{(y/x)} = p^{(x/y)} = 0.15$) terminations, respectively (from Meza-Fajardo & Papageorgiou, 2008).

4. ACCURACY ANALYSIS

In this section the accuracy of the M-PML is studied by means of numerical examples. The problem of the propagation of a P-wave on an isotropic elongated domain of the previous section is again considered. In order to assess the effect of the PML terminations on the solution, receivers are placed at the same x-coordinate of the source and at distances of 0.15, 0.25, 0.35, 0.5, 0.7, 1.0, 2.0, 3.0, 6.0, 7.0, 7.5, 8.0, and 8.5 km from the source in the direction of the y-coordinate. For a cylindrical wave, the x-component of the exact solution for velocity at those locations is zero, and therefore, the component obtained in the simulation is a measure of the error due to the presence of the absorbing layers. The energy reflected due to the absorbing boundaries was then assessed by comparing the x-component of the velocity with the y-component in the following manner:

$$\frac{\|V_x\|}{\|V_y\|} = \frac{\sqrt{\int_0^T {V_{x1}}^2 dt}}{\sqrt{\int_0^T {V_{y1}}^2 dt}} \tag{4.1}$$

Simulations were performed for different values of the ratios $d_0/f_d =$ 1, 5, 10, 15, 20 and $H/\lambda =$ 0.5, 1, 1.5, 2, where d_0 is the maximum value of damping, H is the absorbing layer width, and λ is the wavelength associated to the dominant frequency f_d.

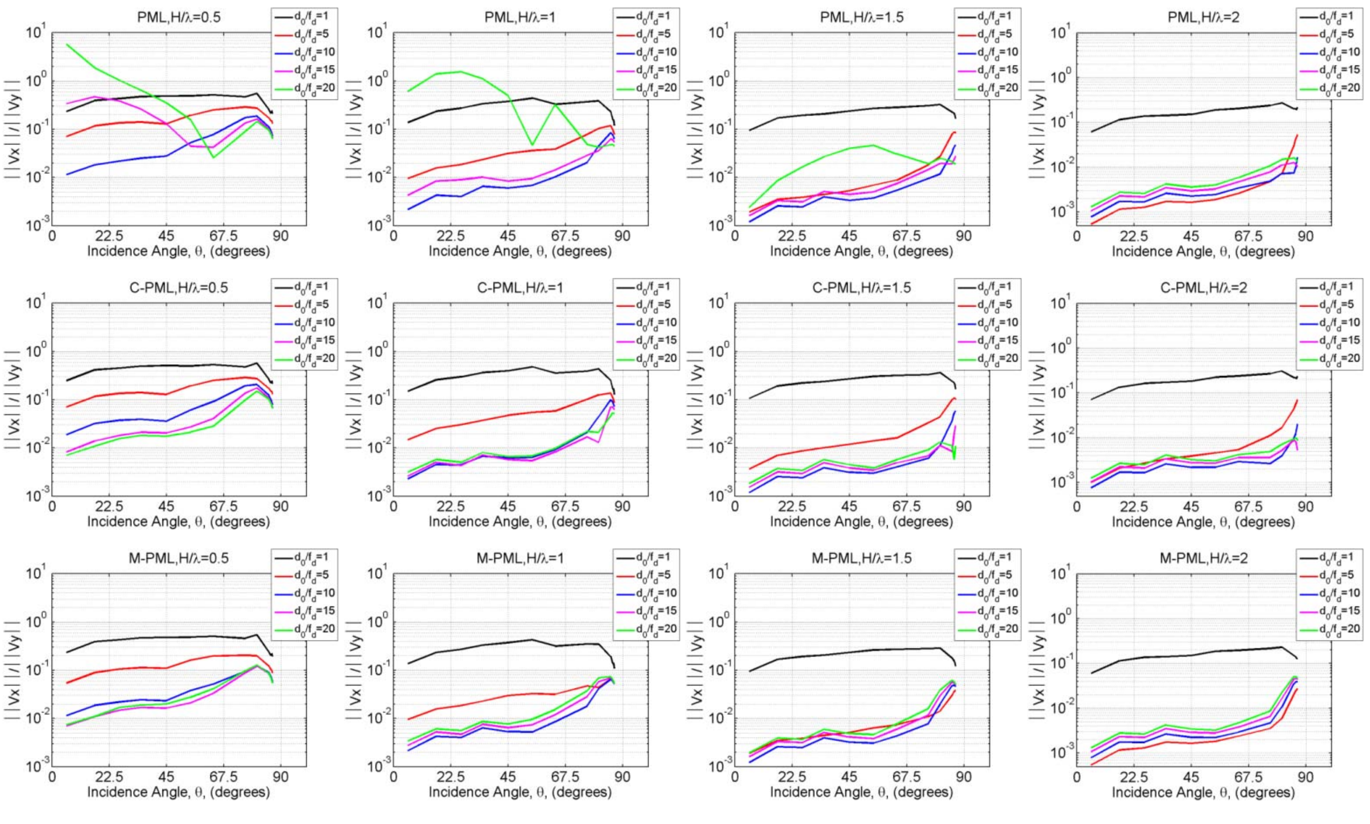

Figure 5. Reflection of energy for an incident P-wave vs. angle of incidence for PML terminations (top row), C-PML terminations (middle row) and M-PML terminations (bottom row).

Figure 5 illustrates the reflections obtained in simulations with classical PML, C-PML and M-PML terminations. The results clearly show that for a fixed value of H/λ, the C-PML and M-PML give better results (smaller reflections) when $d_0/f_d > 1$. In general, the reflections due to the C-PML and M-PML appear to be of the same order of magnitude. The value $d_0/f_d = 1$ seems to provide too little damping in the absorbing layer to efficiently absorb the waves and prevent large reflections. The large reflections observed at small incidence angles in the classical PML, for values $d_0/f_d \sim 15 - 20$ are a result of the spurious waves (due to the instability of the PML) which contaminate the solution. This is related to the fact that the higher the ratio d_0/f_d, the earlier the instability contaminates the solution. It can be also observed that the ratio H/λ has more impact on reducing reflections than the ratio d_0/f_d. The fact that reflection is reduced by increasing the ratio H/λ implies that reflections due to discrete classical PML, C-PML and M-PML terminations are frequency-dependent.

REFERENCES

Adhikari, S., Friswell, M.I. (2001). Eigenderivative analysis of asymmetric non-conservative systems. *International Journal for Numerical Methods in Engineering* **51**, 709-733.

Bécache, E., Fauqueux, S., Joly, P. (2003). Stability of perfectly matched layers, group velocities and anisotropic waves. *Journal of Computational Physics* **188**, 399-433.

Bécache, E., Petropoulos, P.G., Gedney, S.D. (2004). On the long-time behaviour of unsplit Perfectly Matched Layers. *IEEE Transactions on Antennas and Propagation* **52:5**, 1335-1342.

Bérenger, J.P. (1994). A Perfectly Matched Layer for the absorption of electromagnetic waves. *Journal of Computational Physics* **114**, 185-200.

Chew, W.C., Weedon W. (1994). A 3D perfectly matched medium from modified Maxwell's equations with stretched coordinates. *Microwave and Optical Technology Letters* **7:13**, 559-604.

Festa G., Delavaud, E., Vilotte, J.P. (2005). Interaction between surface waves and absorbing boundaries for wave propagation in geological basins: 2D numerical simulations. *Geophysical Research Letters* **32**, L20306, doi:10.1029/2005GL024091.

Festa G., Vilotte J.P. (2005). The Newmark scheme as velocity-stress time staggering: an efficient PML implementation for spectral element simulations of elastodynamics. *Geophysical Journal International* **161**, 798-812.

Gallina, P. (2003). Effect of Damping on Asymmetric Systems. *Journal of Vibration and Acoustic* **125**, 359-364.

Hinrichsen, D., Pritchard, A.J. (2005). Mathematical Systems Theory I. Modelling, State Space Analysis, Stability and Robustness. Springer-Verlag.

Komatitsch, D., Martin R. (2007). An unsplit convolutional Perfectly Matched Layer improved at grazing incidence for the seismic wave equation. *Geophysics* **72:5**, SM155-SM167.

Komatitsch, D., Tromp J. (2003). A perfectly matched layer absorbing boundary condition for the second-order seismic wave equation. *Geophysical Journal International* **154**, 146-153.

Kuzuoglu, M., Mittra, R. (1996). Frequency Dependence of the Constitutive Parameters of Causal Perfectly Matched Anisotropic Absorbers. *IEEE Microwave and Guided Wave Letters* **6:12**, 447-449.

Meza-Fajardo K. C. (2007). Numerical Simulation of Wave Propagation in Unbounded Elastic Domains using the Spectral Element Method, *PhD Thesis*, Università degli Studi di Pavia, ROSE School, Pavia, Italy.

Meza-Fajardo K. C. (2008). A Non-Convolutional Perfectly Matched Layer for Isotropic Elastic Media, *Individual study*, Università degli Studi di Pavia, ROSE School, Pavia, Italy.

Meza-Fajardo, K. C. and A. S. Papageorgiou (2008). A Non-Convolutional, Split-Field Perfectly Matched Layer (PML) For Wave Propagation In Isotropic And Anisotropic Elastic Media - Stability Analysis, *Bulletin of the Seismological Society of America* **98:4**, (to appear).

Teixeira, F.L., Chew, W. C. (1999). On causality and Dynamic Stability of Perfectly Matched Layers for FDTD Simulations. *IEEE Transactions on Microwave Theory and Techniques* **47:6**, 775-785.